Cerebral Cortex, June 2016;26: 2517–2529

doi: 10.1093/cercor/bhv078
Advance Access Publication Date: 15 May 2015
Original Article

ORIGINAL ARTICLE

Defects During *Mecp2* Null Embryonic Cortex Development Precede the Onset of Overt Neurological Symptoms

Francesco Bedogni[1], Clementina Cobolli Gigli[1,2], Davide Pozzi[3], Riccardo Lorenzo Rossi[4], Linda Scaramuzza[1], Grazisa Rossetti[4], Massimiliano Pagani[4], Charlotte Kilstrup-Nielsen[2], Michela Matteoli[3,5], and Nicoletta Landsberger[1,2]

[1]San Raffaele Rett Research Unit, Division of Neuroscience, San Raffaele Scientific Institute, 20132 Milan, Italy, [2]Laboratory of Genetic and Epigenetic Control of Gene Expression, Division of Biomedical Research, Department of Theoretical and Applied Sciences, University of Insubria, Busto Arsizio, 21052 Varese, Italy, [3]Laboratory of Pharmacology and Brain Pathology, Humanitas Clinical and Research Center, Rozzano, 20089 Milan, Italy, [4]Istituto Nazionale di Genetica Molecolare "Romeo ed Enrica Invernizzi", 20122 Milan, Italy, and [5]Dip di Biotecnologie Mediche e Medicina Traslazionale, Università di Milano, Milan, Italy

Address correspondence to Nicoletta Landsberger, SRRRC, Via Olgettina, 58, 20132 Milan, Italy. Email: landsberger.nicoletta@hsr.it

Clementina Cobolli Gigli, Davide Pozzi, and Riccardo Lorenzo Rossi equally contributed to this work.

Abstract

MeCP2 is associated with several neurological disorders; of which, Rett syndrome undoubtedly represents the most frequent. Its molecular roles, however, are still unclear, and data from animal models often describe adult, symptomatic stages, while MeCP2 functions during embryonic development remain elusive. We describe the pattern and timing of *Mecp2* expression in the embryonic neocortex highlighting its low but consistent expression in virtually all cells and show the unexpected occurrence of transcriptional defects in the *Mecp2* null samples at a stage largely preceding the onset of overt symptoms. Through the deregulated expression of ionic channels and glutamatergic receptors, the lack of Mecp2 during early neuronal maturation leads to the reduction in the neuronal responsiveness to stimuli. We suggest that such features concur to morphological alterations that begin affecting *Mecp2* null neurons around the perinatal age and become evident later in adulthood. We indicate MeCP2 as a key modulator of the transcriptional mechanisms regulating cerebral cortex development. Neurological phenotypes of *MECP2* patients could thus be the cumulative result of different adverse events that are already present at stages when no obvious signs of the pathology are evident and are worsened by later impairments affecting the central nervous system during maturation and maintenance of its functionality.

Key words: embryonic cerebral cortex development, intrinsic neuronal excitability, MeCP2 null cortex, neurological disorders, transcriptome

Introduction

Rett syndrome (RTT) is a devastating genetic disorder that worldwide represents the most common genetic cause of severe intellectual disability in females. Typical RTT patients appear to develop normally throughout the first 6–18 months of life when neurological development arrests and a regression phase leads to the loss of previously acquired skills. During and after the regression phase, patients develop a host of typical symptoms

including intellectual disabilities, respiratory problems, hand stereotypies, absence of speech, and epilepsy. Genetic analyses show that most RTT cases are caused by mutations in the *MECP2* gene. Moreover, the same gene is less frequently associated with neonatal encephalopathy and *MECP2* duplication syndrome in males, and, in both genders, with autism, schizophrenia, Angelman-like syndrome, and mild to severe mental retardation (Amir et al. 1999; Bienvenu et al. 2000; Yusufzai and Wolffe 2000; Chen et al. 2001; Guy et al. 2001). All in all, such molecular data suggest that MeCP2 is a key protein in the brain, where its levels and functions cannot be altered without severe consequences.

The generation of several mouse models carrying different *Mecp2* alterations has been instrumental to investigate MeCP2 functions and their involvement in pathogenic mechanisms. In particular, the so far mostly used *Mecp2* null male appears normal until 3–4 weeks of age, when it develops gross abnormalities such as hind limb clasping, stiff and uncoordinated gait, hypotonia, reduced spontaneous movements, tremor, breathing irregularities, and often, seizures (Ricceri et al. 2008). *Mecp2* null brain displays several structural abnormalities, including smaller size (Belichenko et al. 2008), while studies focusing in deeper details on brain cellular architecture showed that *Mecp2* null neurons display reduced soma size, changes in density, size and morphology of dendritic spines, as well as in the orientation of axons (Smrt et al. 2007; Belichenko et al. 2009). Accordingly, many studies have shown that *Mecp2* null hippocampal slices are characterized by significant deficits in synaptic transmission (Asaka et al. 2006; Zhang et al. 2008), as well as in synaptic plasticity (Della Sala and Pizzorusso 2014). Interestingly, ablation of *Mecp2* in adulthood results in defects of neuronal functions resembling those displayed by animals constitutively missing Mecp2 (Gemelli et al. 2006; Fyffe et al. 2008; McGraw et al. 2011; Cheval et al. 2012; Nguyen et al. 2012). Altogether, these conditional animal models indicate that MeCP2 must play a role in the maintenance of brain functionality at post-natal ages. On the contrary, the investigation of the possible roles played by Mecp2 during embryonic development has been largely neglected, although it is now generally accepted that subtle but consistent impairments are present even at early post-natal ages, when typical symptoms are not yet overt (Nomura 2005; Picker et al. 2006; Chao et al. 2007; Santos et al. 2007; Fehr et al. 2011). Moreover, as already alluded, hemizygous *MECP2* male patients display a severe pathological condition as early as at birth (Schüle et al. 2008; Fu et al. 2014), while MeCP2 null neurons derived from induced pluripotent stem cells (iPSCs) display defective structural and functional maturation (Marchetto et al. 2010; Okabe et al. 2010; Kim et al. 2011; Li et al. 2011; Farra et al. 2012).

The present study aims at defining MeCP2 expression pattern and roles in the embryonic cortex and at identifying the temporal windows through which lack of the protein leads to defects that could anticipate the impairments detected later in adulthood. The data presented here provide evidence that MeCP2 plays a pivotal role during cerebral cortex maturation. By analyzing global gene expression in the embryonic neocortex, we show the deregulation of several molecular pathways delaying maturation of *Mecp2* null cortexes and impairing intrinsic neuronal responsiveness to external stimuli. Such early abnormalities, associated with the appearance of morphological defects, worsen during development, persist at later stages, and likely contribute to postnatal cortical functional defects. We hypothesize that, if properly unveiled and characterized, these impairments could, in principle, be exploited as possible early targets for either diagnosis or treatment.

Materials and Methods

Animals and Tissues

The *Mecp2* null mouse strain, originally purchased from Jackson Laboratories (003890 B6.129P2(C)-Mecp2<tm1.1Bird>/J), was backcrossed and maintained on a clean CD1 background; these mice recapitulate the typical phenotype of the regular Black6 original mice, with the advantage of having a larger progeny. Mice genotypes were analyzed through PCR on genomic DNA purified from tails. The following primers, based on published sequences (Miralvès et al. 2007), were used for genotyping: 5′-ACCTAGCCTGCCTGTACTTT-3′ forward primer for null allele; 5′-GACTGAAGTTACAGATGGTTGTG-3′ forward primer for wild type allele; 5′-CCACCCTCCAGTTTGGTTTA-3′ as common reverse primer. Time-pregnant females were generated by overnight crossing wild type CD1 males with $Mecp2^{+/-}$ heterozygous CD1 females; the day of vaginal plug was considered E0.5. For RNA processing, embryos were collected from anesthetized (Avertin, Sigma-Aldrich), time-pregnant females; dissected cortexes were then rapidly frozen on dry ice and stored at −80 °C. Embryos dedicated to histology were transcardially perfused with 4% PFA under a dissection microscope and post-fixed in 4% PFA for additional 4 h; about 12 μm cryosections were then stored at −80 °C until further analysis. All procedures were performed in accordance with the European Community Council Directive 86/609/EEC for care and use of experimental animals; all the protocols were approved by the Italian Minister for Scientific Research and by the local Animal Care Committee.

Histology

About 12 μm sections were washed in PBS, treated to retrieve antigens (when necessary), and incubated for 1 h in blocking solution (10% horse serum, 0.1% Triton X-100, and PBS). Tissues were then incubated with the primary antibody diluted in blocking solution overnight at 4 °C. Primary antibodies were used at the following concentrations: anti-Mecp2 (1 : 1000; Sigma-Aldrich, M9317), anti-Mecp2 (1 : 200; Cell Signaling, D4F3), anti-Nestin (1 : 200; Millipore, MAB353), anti-Tuj1 (1 : 2000; Covance, MMS-435P), anti-Reelin (1 : 20; DSHB, R4B), anti-GFAP (1 : 300; Cell Signaling, GA5), and anti-GFP (1 : 1000; Molecular Probe, A10262). For bright field imaging, after incubation with biotinylated secondary antibodies (Vector Laboratory), sections were treated with the Vector ABC kit (Vectastain) followed by staining with the Vector VIP peroxidase substrate kit. For fluorescent imaging, Alexafluor secondary antibodies were applied for 2 h at room temperature; sections were then counterstained with DAPI (Invitrogen) and mounted in Prolong Gold (Invitrogen). Nikon microscopes, objectives, and software were used for imaging, and panels were composed into figures using Adobe Photoshop.

Neurosphere Generation

The procedure to generate neural stem cell (NSC) culture was first described by Gritti et al. (1996); our protocol is based on the one described by Magri et al. (2011). Briefly, E15.5 embryos were individually dissected in PBS and the neocortex was transferred in Dulbecco's Modified Eagle Medium/F12 (DMEM) and dissociated by extensive enzymatic digestion with Papaine (Sigma). Cells were then grown in medium containing DMEM/F12, 0.66% glucose, L-glutamine 1%, Pen/Strep 1%, 4 μg/mL of heparin, hormone mix, and also with the addition of either 20 ng/mL epidermal growth factor and 10 ng/mL basic fibroblast growth factor or bFGF alone. In such conditions, cells spontaneously formed

neurospheres (Gritti et al. 1996). Neurospheres were then dissociated in single-cell cultures and plated on matrigel-coated coverslips (BD Bioscience). Differentiation was obtained by replacing growth factors with 2% serum. PFA fixation was used to produce samples to be analyzed by immunofluorescence experiments once the culture reached desired cell density, otherwise total RNA was purified as described below.

RNA Purification, cDNA Synthesis, Microarray, and qPCR Analysis

Total RNA was purified either from cultured neurospheres, neurons, or embryonic cortexes using commercial kits (RNeasy Mini and Micro Kit, QIAGEN) following vendor's protocols. Cortexes collected for the microarray analysis were obtained from 3 wild type and 3 *Mecp2* null E15.5 animals. Isolated total RNA quality was checked for integrity with 2100 Bioanalyzer (Agilent Technologies); samples with RNA integrity number lower than 8 were discarded. Gene expression of whole transcriptome was performed with Illumina Direct Hybridization Assays according to the standard protocol (Illumina). For each sample, 500 ng of total RNA were reverse-transcribed according to the Illumina TotalPrep RNA Amplification kit (Ambion) and cDNA was generated. Washing, staining, and hybridization were performed according to the standard Illumina protocol; each sample was hybridized onto Illumina MouseRef-8 Expression BeadChip arrays. Hybridization and scanning were performed according to the manufacturer's indications on an Illumina iScan System, and data were processed with GenomeStudio; array data were processed with quantile normalization in the Genome Studio software before further analysis. Average signals were calculated on gene-level data according to the standard Illumina detection cutoff (detection *P*-value <0.001). RNA dedicated to qPCR was retro-transcribed using the RT^2 First Strand Kit (QIAGEN). qPCR results depicted in Figures 1, 3, 5, 6, and 7 were performed using SYBR green (Life Technology) as a fluorescent dye; primers are listed in Supplementary Fig. 8. The results depicted in Figure 4 were obtained using either Neuronal Ion Channels RT^2 Profiler PCR Array or Synaptic Plasticity RT^2 Profiler PCR Array (QIAGEN) following vendor's recommendations.

Gene Set Enrichment Analysis

To analyze microarray results, the gene set enrichment analysis (GSEA) was used. The 2 lists of expression values (one for the *Mecp2* null phenotype and one for the wild type phenotype) were inserted in the GSEA software, first ranking genes on the base of their expression values and then determining the distribution of a set of genes (gene set) throughout the ranked list (www.broadinstitute.org; Subramanian et al. 2005). To obtain a numerical measurement of the degree by which a gene set of interest is more represented in one experimental group or the other, the software calculates an enrichment score (ES). The ES increases when a gene that belongs to a gene set is found in the ranked list, or decreases when the gene is not in the gene set. The degree of the increment (or decrement) depends on

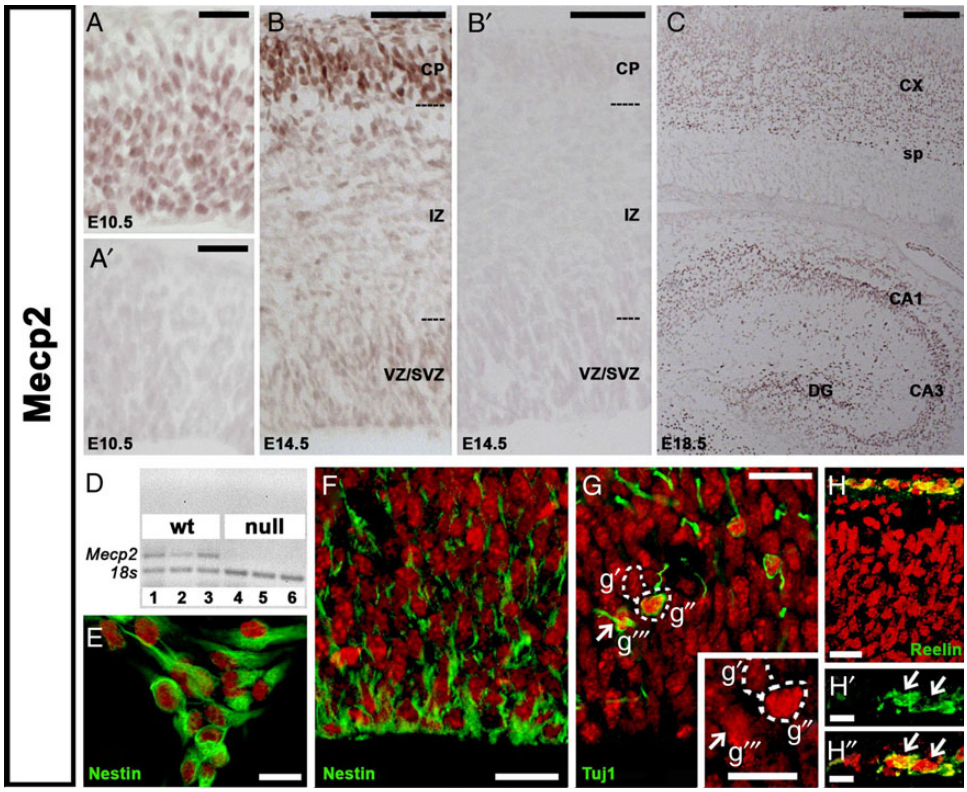

Figure 1. Different levels of Mecp2 can be detected in each cell type populating the developing embryonic neocortex. Weak but specific Mecp2 levels of expression are detected in progenitors populating the neuroepithelium (E10.5; *A* and *A′*) and the VZ and SVZ (E14.5; *B*, *B′*, and *F*) and in cultured neuroprogenitors through qPCR analysis of *Mecp2* transcription (*D*) and immunofluorescence (*E*). In *G*, Mecp2 levels increase according to the maturity of the cell: Tuj1$^+$ cells (g″ and g‴) show higher levels compared with the Tuj1$^-$ cell in g′. Highest levels of Mecp2 are detected in the CP (*B* and *C*) and in CR cells (*H*, *H′*, and *H″*). In *D*, numbers identify conditions of NSCs grown with epidermal growth factor and bFGF (1 and 4); bFGF alone (2 and 5), or serum (3 and 6). IZ: intermediate zone; CP: cortical plate; VZ: ventricular zone; SVZ: subventricular zone; CX: cortex; sp: subplate; CA1 and 3: Cornu Ammoni 1 and 3; DG: dentate gyrus. Scale bars: C: 100 μm; B/B′: 50 μm; A/A′/F/G/H: 25 μm; E/H′/H″: 10 μm.

the amplitude of differential expression in the analyzed dataset. The next step performed by the GSEA is to assess the statistical significance of the ES, determining the nominal *P*-value by an empirical gene set-based permutation test procedure. Gene sets are chosen by the users, they can derive from a custom-made list of genes, or can be downloaded from MSigDB (Molecular Signature Database; Subramanian et al. 2005).

We produced the gene sets described in Figure 2 using published data (Ayoub et al. 2011) where the authors micro-dissected the E14.5 cortex into 3 different groups including ventricular zone (VZ), subventricular zone (SVZ)–intermediate zone (IZ), and cortical plate (CP), and separately analyzed their transcriptional profile through RNA sequencing (RNA*seq*). To identify genes exclusively expressed in the proliferative compartment or in the late post-mitotic neurons populating the CP, expression data were downloaded and fold change values calculated between the VZ and the CP datasets. Setting a cutoff value at 20 folds, we obtained 221 genes exclusively expressed in the proliferative compartment and 162 genes specifically expressed in late post-mitotic neurons. To be noticed, the gene set defining the proliferative identity is comprehensive of genes expressed at different levels in both the VZ and SVZ, as laser dissection does not enable separating a mixed population such as the one composing the VZ/SVZ. This is demonstrated by the presence in the VZ of levels of expression of Eomes (Tbr2; Supplementary Fig. 1) a gene defining intermediate progenitor cells composing the SVZ (Englund et al. 2005). The results described in Table 1 and Supplementary Fig. 3 were obtained using canonical pathway gene sets (C2, curated gene sets, comprehensive of information from the database BIOCARTA, KEGG, and REACTOME; www.broadinstitute.org).

Neuronal Cultures

E15.5 cortexes were isolated, washed in HBSS, digested with Trypsin 0.25%, and mechanically dissociated by pipetting. Cells were plated on poly-L-lysine 0.1 mg/mL at low density 30 000 cells/well in a 6-multiwell plate each containing a 24-mm diameter glass coverslip. Neurons were grown in culture medium

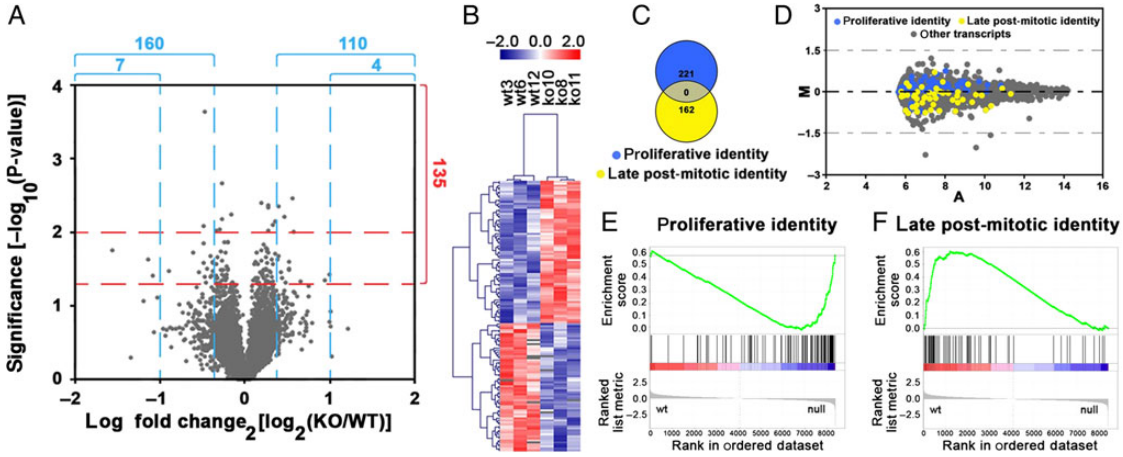

Figure 2. E15.5 *Mecp2* null neocortexes display mildly perturbed transcriptional profiles. Volcano plot (*A*) displays statistical significance versus differential expression (log fold change), blue lines delimitate the 1.3- and 2.0-fold change cutoffs, and red lines correspond to *P*-values of 0.05 and 0.01 (1.3 and 2 accordingly in the inverse log scale). The heatmap (*B*) shows that the 135 deregulated genes selected according to their statistical significance (*P*-value <0.05) separate wild type and null samples. Genes were clustered according to Pearson distance metric, individual expression values rendered in $\log_2$ transformed *z*-scores. In *C*–*F*, GSEA suggests a delay in maturation affecting the *Mecp2* null neocortex. The 2 gene sets identifying the proliferative compartment and the late post-mitotic neurons are not overlapping (Venn's diagram in *C*) and segregated in either wild type or null samples [MA plot, M: $\log_2$(KO/WT); A: $0.5 \times \log_2$(KO × WT)]. In *E* and *F*, the GSEA results using such gene sets are depicted, and the list of the genes composing the 2 gene sets can be found in Supplementary Fig. 2.

Table 1 List of gene sets enriched in the WT samples

Gene sets	SIZE	ES	Nominal *P*-value
REACTOME_TRAFFICKING_OF_AMPA_RECEPTORS[a]	18	0.68	0E+00
REACTOME_ION_CHANNEL_TRANSPORT[c]	21	0.66	0E+00
REACTOME_PHOSPHOLIPASE_C_MEDIATED_CASCADE[b]	22	0.66	0E+00
REACTOME_POTASSIUM_CHANNELS[c]	30	0.60	0E+00
REACTOME_G_ALPHA_I_SIGNALLING_EVENTS[b]	47	0.53	0E+00
REACTOME_PLC_BETA_MEDIATED_EVENTS[b]	21	0.64	0E+00
REACTOME_CA_DEPENDENT_EVENTS[c]	16	0.66	0E+00
REACTOME_UNBLOCKING_OF_NMDA_RECEPTOR_GLUTAMATE_BINDING_AND_ACTIVATION[a]	7	0.83	0E+00
REACTOME_SIGNALING_BY_GPCR[b]	178	0.38	0E+00
KEGG_CALCIUM_SIGNALING_PATHWAY[c]	61	0.53	2E–03
KEGG_PHOSPHATIDYLINOSITOL_SIGNALING_SYSTEM[b]	43	0.54	2E–03
REACTOME_RAS_ACTIVATION_UPON_CA2_INFLUX_THROUGH_NMDA_RECEPTOR[a]	7	0.81	2E–03
REACTOME_DAG_AND_IP3_SIGNALING[b]	17	0.67	4E–03
REACTOME_VOLTAGE_GATED_POTASSIUM_CHANNELS[c]	13	0.70	4E–03

Note: Such gene sets were chosen for their relevance in neocortex maturation, [a]represents glutamatergic receptors, [b]intracellular effectors and [c]ionic channels.

containing Neurobasal, B-27 (1 : 50), Glutamax 1%, and Pen–Strep 1% (Invitrogen, Carlsbad, CA, USA).

Calcium Imaging

Cortical neurons were loaded with calcium-sensitive dye by incubating in 10 mM Oregon Green 488 BAPTA-1 AM (Molecular Probes) in Neurobasal Medium for 1 h at 37 °C and then imaged for calcium response. Both glutamate and electrical field stimulation were performed in KRH (Krebs'–Ringer's–HEPES) containing (in μM): 125 NaCl; 5 KCl; 1,2 $MgSO_4$; 1,2 KH_2PO_4; 25 HEPES; 6 glucose; 2 $CaCl_2$; pH 7.4. Glutamate stimulation was performed in the presence of Nifedipine 20 μM, Tetrodotoxin (TTX) 1 μM, and Bicuculline 20 μM, by applying 25 μM of glutamate with a perfusion system (Warner Instruments, Hamden, CT, USA). Electrical field stimulation was performed in the presence of 6-cyano-7-nitroquinoxaline-2,3-dione (CNQX) 20 μM, R-2-amino-5-phosphonopentanoate (APV) 50 μM, and Bicuculline 20 μM using a stimulation chamber (Warner Instruments). Electrical-evoked calcium transients were induced with a stimulus train of 2 s (duration 1 ms; amplitude 90 mA) at 30 Hz as previously reported (Pozzi et al. 2013), using a train generation unit (Digitimer Ltd, DG2A) connected to a stimulus isolation unit (SIU-102; Warner Instruments). Recording chambers were placed on the stage of an IX-71 inverted microscope (Olympus, Hamburg, Germany) equipped with an EMCCD (electron-multiplying CCD) camera (Quantem 512 × 512, Photometrics). Illumination was obtained using a light-emitting diode single LED (Cairn Research Optoled; 470 nm) and a related GFP filter; 16-bit images were captured using a ×20 objective (NA: 0.8). Regions of interest (ROIs) of about 15-pixel diameter (corresponding to ~12 μm) were drawn on the cell cytoplasm of virtually all the cells in the recorded field. Time-lapse recording of calcium dynamics was performed with an acquisition rate of 5 Hz for 600 s and off-line analyzed with the MetaFluor software (Molecular Devices). Calcium responses were measured as ΔF ($F_{max} - F_0$) with respect to the baseline (F_0). A total of 10–15 neurons were analyzed for each field. Cumulative data were then analyzed through Kolmogorov–Smirnov statistic to verify non-parametric distribution.

In Utero Electroporation

For in utero electroporation the plasmid pLentiLox3,7 GFP vectors expressing either a short hairpin RNA directed against *Mecp2* (5'-GTCAGAAGACCAGGATCTC-3') or beta-galactosidase (control) were used. Timed-gestation CD1 females (E13.5) were deeply anesthetized with Avertin before exposing uterine horns by midline laparotomy. DNA (1 μg/μL) together with dast green for counterstaining was injected in the telencephalic vesicle using a pulled micropipette, and then platinum electrodes were placed outside the uterus over the telencephalon and a train of four 50 ms squared pulses of 40 V were applied at 1-s interval from each. The uterus was then placed back in the abdomen, and muscle and skin were sutured. Animals were sacrificed at E18.5. Brains were collected by first checking their fluorescence (under a fluorescent stereoscope); fluorescent tissues were then enzymatically disaggregated and sorted on the basis of their fluorescence content (deriving from the expression of GFP). Both GFP^+ and GFP^- cells were collected from animals treated with either LacZ controls or *Mecp2*-directed shRNAs, such that GFP^- cells were used as negative controls for GFP^+ samples deriving from both the experimental groups; total RNA was then purified as already described. Transcriptional levels depicted in Figure 7A are expressed as the percentage of expression versus the GFP^- group (considered 100%, dotted line). Tissues dedicated to histology were handled as already described.

Morphological Analysis

Morphological analyses were performed at DIV3 on cortical neurons (isolated from E15.5 embryos and prepared as described) plated at very low density (30 000 cells/well). Immunofluorescence was performed as previously described using antibodies raised against Tuj1 and DAPI. Neurites length was measured only in neurons not connected with others using the NeuronJ, a plugin of ImageJ. Neurites were considered as the Tuj1-positive structure starting from the soma of each neuron; they were classified as "long" when their length was above 100 μm, or "short" when shorter than 100 μm. 3 null and 4 wild type animals were used for these measurements. The size of neuronal nuclei was measured using ImageJ on images collected from both primary cultures and 12 μm cortical slices from E15 and E18.5 wild type and null animals, and such measurements were based on DAPI staining.

Results

While the profile of Mecp2 distribution in the murine embryonic cerebral cortex has been previously analyzed, no conclusive data highlight whether it is expressed in all the cellular types composing the developing cortex. Several studies suggested that Mecp2 expression is restricted to late post-mitotic neurons residing in the CP and Cajal-Retzius (CR) cells composing the marginal zone, but it is absent from cycling progenitors in the VZ/SVZ (the proliferative compartment) and from maturing neurons in the IZ (Jung et al. 2003; Kishi and Macklis 2004; Schmid et al. 2008). However, the presence of Mecp2 in embryonic stem cells has been suggested in other studies (Caballero et al. 2009; Okabe et al. 2010; Kim et al. 2011). To draw a definitive picture of the pattern and timing of Mecp2 expression during cortical development, we first performed a detailed immunohistochemistry analysis (Fig. 1) using null tissues as negative controls to enable the specific detection of low levels of Mecp2. We revealed the presence of Mecp2 in a large set of cell types, spanning from cortical neuroblasts populating the neuroepithelium at E10.5 (compare Fig. 1A, wild type, with A′, *Mecp2* null), progenitors, immature and differentiated neurons at E14.5 (wild type in Fig. 1B and null in Fig. 1B′), to virtually all the cell types of the cortex at E18.5 (Fig. 1C). The detection of *Mecp2* transcript in proliferating and differentiating NSCs (Fig. 1D), together with the protein co-localization with Nestin (Fig. 1E,F), Tuj1 (Fig. 1G), and Reelin (Fig. 1H), demonstrates that Mecp2 is expressed in a very heterogeneous set of cells. In accordance with published studies (Jung et al. 2003), we found that Mecp2 levels vary according to the stage of cellular maturation (Fig. 1B,G), with $Tuj1^-$ cells in proliferative areas (Fig. 1g′) expressing lower levels of Mecp2 compared with $Tuj1^+$ (Fig. 1g″,g‴).

Given the novel information gained through the analysis of Mecp2 expression in the developing cortex, we then investigated its transcriptional activity by purifying total RNA from both wild type and *Mecp2* null embryonic cortexes collected at E15.5 and screening transcriptional levels through microarray (Fig. 2).

Using fold change as a selection criterion for differential expression, we identified 270 differentially expressed genes with a fold change cutoff of 1.3 and 11 genes with a fold change cutoff of 2 (Fig. 2A). Using a *P*-value of 0.05 as a cutoff criterion, we identified only 135 differentially expressed genes; nevertheless, these 135 differentially expressed genes were able to clearly segregate

the 2 tested conditions (wild type and *Mecp2* null mutants), as shown by the hierarchical cluster heatmap of expression data of the profiled 6 individual samples (Fig. 2*B*). However, using gene ontology (GO) analysis to functionally describe the 2 gene clusters separately (genes up- or downregulated in *Mecp2* null mutant), we were not able to find any GO term enriched at a significant level (Supplementary Fig. 1).

Given that (1) differential expression analysis identified only a limited number of genes; (2) expression variations were only mild in amplitude, probably due to the fact that the neocortex is populated by an heterogeneous set of cell types each expressing specific levels of Mecp2, thus reducing the detection of possible differences in expression; and (3) simple GO analysis was not useful in functionally annotating the selected gene lists, we decided to use the GSEA to explore data in deeper details and extract biological insights. GSEA overcomes common analytical challenges inherent to microarray technology, such as detection noise, that could lead, when differential expression is minimal, to no or few genes passing the threshold for statistically significant results. GSEA takes into account gene sets that likely share common biological functions or regulation; thus, in contrast to single-gene analyses, this approach allows to emphasize the contribution of each expression difference (even mild) in a group of genes that roughly represent the whole molecular pathways (Subramanian et al. 2005).

First, we obtained a custom-made gene set extracted from data presented by Ayoub et al. (2011), in which the authors, through laser dissection and RNA*seq*, profiled transcription either in the VZ, SVZ/IZ, or CP of the E14.5 developing cortex. By setting a fold change cutoff of 20 on the transcriptional ratio of each gene analyzed in the dataset of either VZ or the CP provided by the authors, we identified 2 gene sets exclusively representative of either the proliferative compartment or late post-mitotic neurons (221 and 162 genes, respectively). As shown by the Venn diagram in Figure 2C, the 2 lists are not overlapping (the genes composing them are provided in Supplementary Fig. 2). These 2 groups of genes appeared fairly segregated between the 2 genotypes analyzed in our work (MA plot in Fig. 2*D*) and a significant enrichment (nominal *P*-value <0.001) was accordingly highlighted by analyzing the transcriptional profiling through the GSEA method: the proliferative compartment identity was enriched in the null sample (i.e., up-regulated in the null sample, Fig. 2*E*), whereas, on the contrary, the late post-mitotic identity was enriched in the wild type sample (i.e., downregulated in the null sample, as depicted in Fig. 2*F*). This was a first hint leading us to hypothesize that, in the E15.5 *Mecp2* null cortex, the maturation of newly born cortical neurons might be somehow impaired. These 2 gene sets were chosen a priori to highlight whether one of the two transcriptional identities could be enriched in one of the two genotypes analyzed; in a further analytical approach, we used GSEA in a more canonical way, scanning an entire gene set collection to highlight the enrichment in specific molecular pathways. In order to do that, we superimposed on the wild type versus the null dataset the curated gene sets (C2) of the Molecular Signature Database (MSigDB, version 3.1, comprising 4850 different gene sets; Subramanian et al. 2005). Table 1 summarizes gene sets significantly enriched in the wild type samples (thus reduced in the null cortexes), with a nominal *P*-value cutoff of 0.001. These gene sets were selected because: (i) they all converge in 3 main groups: intracellular effectors, glutamatergic receptors, and ionic channels ([a,b,c] in Table 1); (ii) such mechanisms are all crucial for neuronal physiology, and (iii) they were all grouped at the top of the list ranked according to statistical significance (Supplementary Fig. 3 depicts all the gene sets showing a nominal *P*-value <0.001). Of interest, these pathways all share the ability to interact with and activate many other downstream effectors. To obtain a first degree of confirmation concerning the possible deregulation of such highlighted pathways, we measured, through qPCR, the levels of transcription of the most representative genes composing each gene set. As illustrated in Figure 3, the transcription levels of different genes common to each of the gene sets depicted as b in Table 1 were down-regulated at E15.5; notably, such down regulation persisted in most cases at later time points (E18.5 and P8).

Because our GSEA results suggested that *Mecp2* might impact the transcription of different glutamate receptors and ion channels (Table 1 [a] and [c]), we measured the cortical expression levels of AMPA, NMDA and metabotropic glutamatergic receptor subunits, whose expression is critical for proper activity-dependent signaling (Lujàn et al. 2005; Uchino et al. 2010; Guo et al. 2013).

We found that the levels of mRNAs encoding for ionotropic receptor subunits were significantly downregulated at both E15.5 and later time points in the null cortex when compared with wild type (Fig. 4). The transcriptional levels of metabotropic receptor subunits (not yet expressed at E15.5; Luján et al. 2005; Ayoub et al. 2011) were mostly normal at E18.5, whereas the expression of some of them (*Grm3*, 5, and 7) was downregulated at P8 in null mice. Similarly, mRNAs for different classes of ion channels (Ca^{2+}, Cl^{-}, K^{+}, and Na^{+}) were downregulated at E15.5 (Fig. 4), and again, such downregulation persisted at later stages of development (E18.5 and P8). Besides the deregulation of gene sets describing the glutamatergic phenotype, we found that gene sets describing GABAergic transmission were mildly enriched in wild type samples. Such effect was not confirmed by qPCR at E15.5 or E18.5, while some downregulation was detected at later time points (P8, Supplementary Fig. 4).

Taken together, our data indicate the occurrence of a fairly long-lasting impairment in the transcriptional regulation of genes involved in neuronal excitability. This may suggest that mechanisms modulating intracellular responses might be impaired in null mice as early as during embryonic neocortical

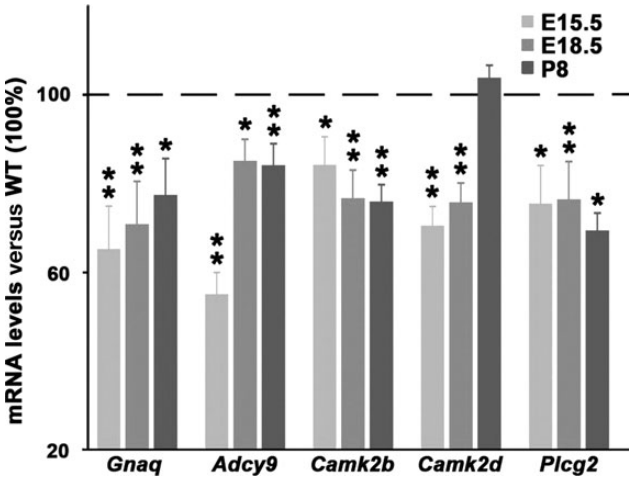

Figure 3. *Mecp2* null embryonic cortexes display the deregulation of many genes involved in many aspects of neuronal physiology. qPCRs results show the downregulation of specific genes in Mecp2 null mice at different developmental stages. Data are expressed as percentage versus wild type (100%, dotted line) ± SEM. $^{*}P < 0.05$; $^{**}P < 0.01$; $N = 8$. *Gnaq*: guanine nucleotide-binding protein (G protein), q polypeptide; *Adcy9*: adenylate cyclase 9; *Camk2B*: calcium/calmodulin-dependent protein kinase II beta; *Camk2D*: calcium/calmodulin-dependent protein kinase II delta; *Plcg2*: phospholipase C, gamma 2 (phosphatidylinositol-specific).

development, and that such defects persist at later time points. To address this point, we produced cultures of cortical neurons established from E15.5 embryos. Neurons were cultured at low density (see Materials and Methods for details), in order to avoid (at least until DIV12) the establishment of a dense interconnected network and to focus on features ascribable, for the most part, to cell autonomous mechanisms. Moreover, by establishing neuronal cultures from E15.5 embryos, we drastically reduced the presence of glial cells, as clearly shown by the immunofluorescence analysis shown in Figure 5A,B, where no GFAP signal is detected and each cell, identified by DAPI staining, is a Tuj1-positive neuronal cell. These cultures were assayed at DIV3 through qPCR

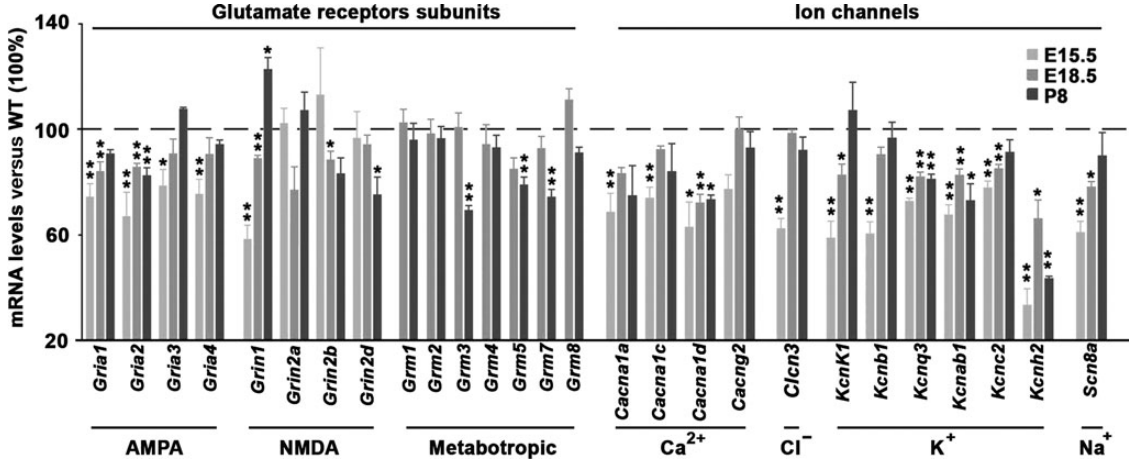

Figure 4. *Mecp2* null cortexes display a persisting transcriptional deregulation of subunits composing either glutamatergic receptors (ionotropic and metabotropic) or ionic channels. qPCR results are expressed as percentage versus wild type (100%, dotted line) ± SEM. *$P < 0.05$; **$P < 0.01$, $N = 4$.

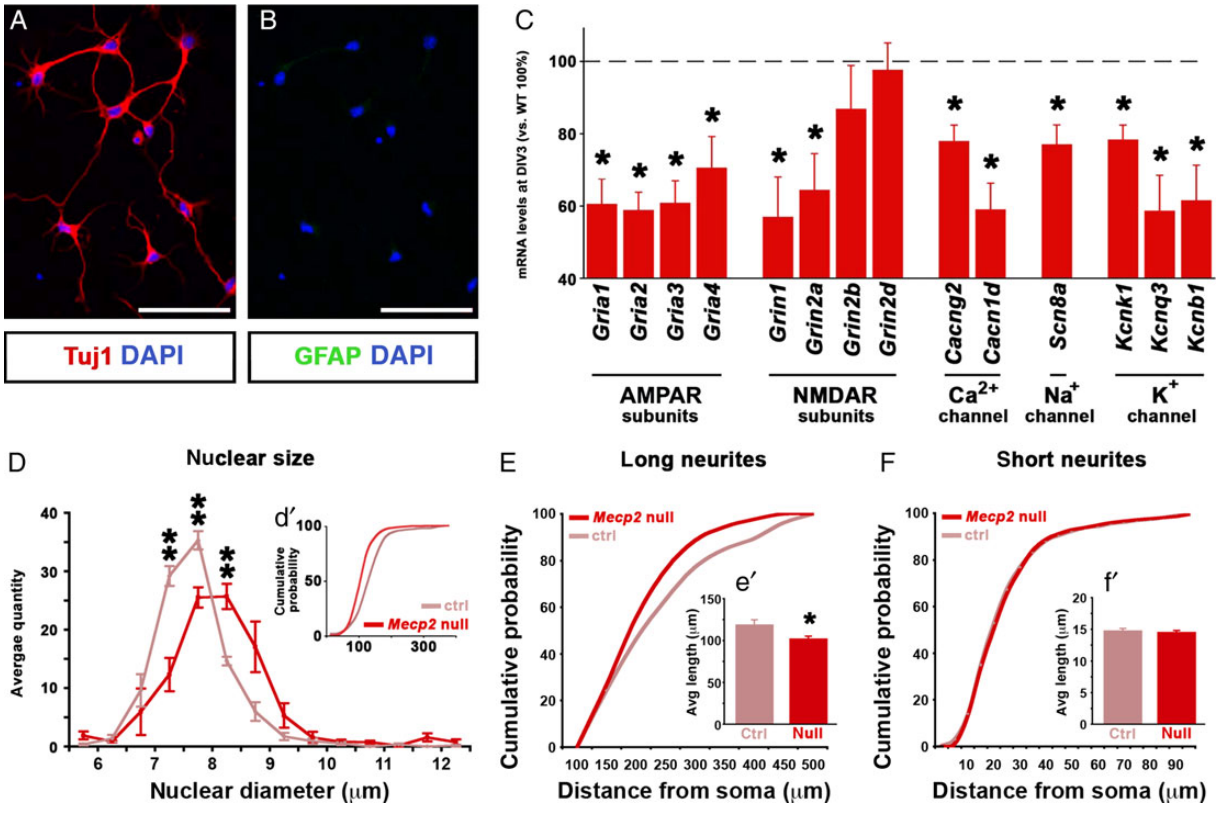

Figure 5. *Mecp2* null cultured neurons recapitulate much of the transcriptional derangement highlighted in Figure 4 and display morphological defects as early as at DIV3. (*A* and *B*) Immunofluorescence analysis of primary cultures established from cortexes at E15.5 shows the virtual absence of glial cells. (*C*) The transcription levels of different glutamatergic receptor and ionic channel subunits were analyzed at DIV3; data are expressed as the percentage of null versus wild type (100%, dotted line) ± SEM. * $P < 0.05$; $N = 5$. (*D* and *E*) Morphological analysis highlighting the reduction in null neurons of both nuclear size (*D*) and average length of long neurites (longer than 100 μm, *E*); short neurites appear unaffected (*F*). Cumulative analysis graphs (in d′ and e′) depict a divergence between groups of 29.3% (d′) and 12.7% (e′); Kolmogorov–Smirnov testing revealed a *P*-value <0.001 for d′ and <0.05 for e′. The cumulative analysis depicted in f′ reveals no significant differences in the number of short (shorter than 100 μm) neurites between wild type and null neurons. Scale bars in *A* and *B*: 50 μm. ** $P < 0.01$; *$P < 0.05$.

in order to evaluate the transcriptional levels of different subunits of AMPA and NMDA receptors as well as Ca^{2+}, Cl^{-}, K^{+}, and Na^{+} channels. We found that the expression of these genes was significantly reduced in null neurons (Fig. 5C), thus in vitro confirming the in vivo data depicted in Figure 4. Interestingly, at such an early stage of differentiation, null cultured neurons display a significant reduction in nuclear size, as shown in Figure 5D. Such observation was only partially reproduced in vivo, where a mild, statistically not significant tendency toward the reduction in nuclear size was observed in null cortexes at E18.5 (Supplementary Fig. 5A; the effect is even milder at E15.5, Supplementary Fig. 5B). Morphological analyses using Tuj1 as a marker of neuronal structures revealed that in vitro neurites longer than 100 μm are on average shorter in null neurons compared with wild type (Fig. 5E), whereas no differences were detected in the length of short neurites (shorter than 100 μm; Fig. 5F).

Next, we used in vitro intracellular Ca^{2+} transients as readout of neuronal responsiveness to chemical and electrical stimulation of cortical primary neurons at early developmental stages. These experiments thus represent a second and functional validation of the GSEA predictions. At first, we characterized calcium responses of DIV3 neurons derived from wild type E15.5 embryos to either glutamate (25 μM; Fig. 6A) or electric stimulation (2 s at 30 Hz; Fig. 6B; Supplementary Fig. 6 depicts typical fields of view with ROI). Ca^{2+} responses evoked by glutamate stimulation (panel a) were strongly reduced by adding CNQX (AMPA receptors blocker, panel a′), and completely abolished by adding both CNQX and the NMDA receptors blocker APV (panels a″). The quantitative analysis of calcium changes, shown in panel a‴, clearly indicates that the glutamate-evoked calcium transients are due to ionotropic receptor activation, with AMPA receptors being responsible for most of the response. This observation implies that ionotropic receptors are predominant over metabotropic receptors in mediating glutamate-induced responses. On the other hand, electrically evoked calcium transients (Fig. 6B, panel b) are strongly reduced by the L-type Ca^{2+} blocker Nifedipine (b′; 20 μM) and completely abolished by 1 μM TTX (b″; Pozzi et al. 2013). The quantitative analysis (panel b‴) indicates that, at this developmental stage, L-type channels represent one of the major channel subtypes driving electrically evoked responses (Pravettoni et al. 2000), and that their opening is completely due to the activation of voltage-dependent sodium channels.

To assess whether the described transcriptional alterations (Figs 3–5) were associated with functional impairment, Ca^{2+} responses evoked by either glutamate or electrical stimulation were analyzed in wild type and null cultured neurons (Fig. 6C–J).

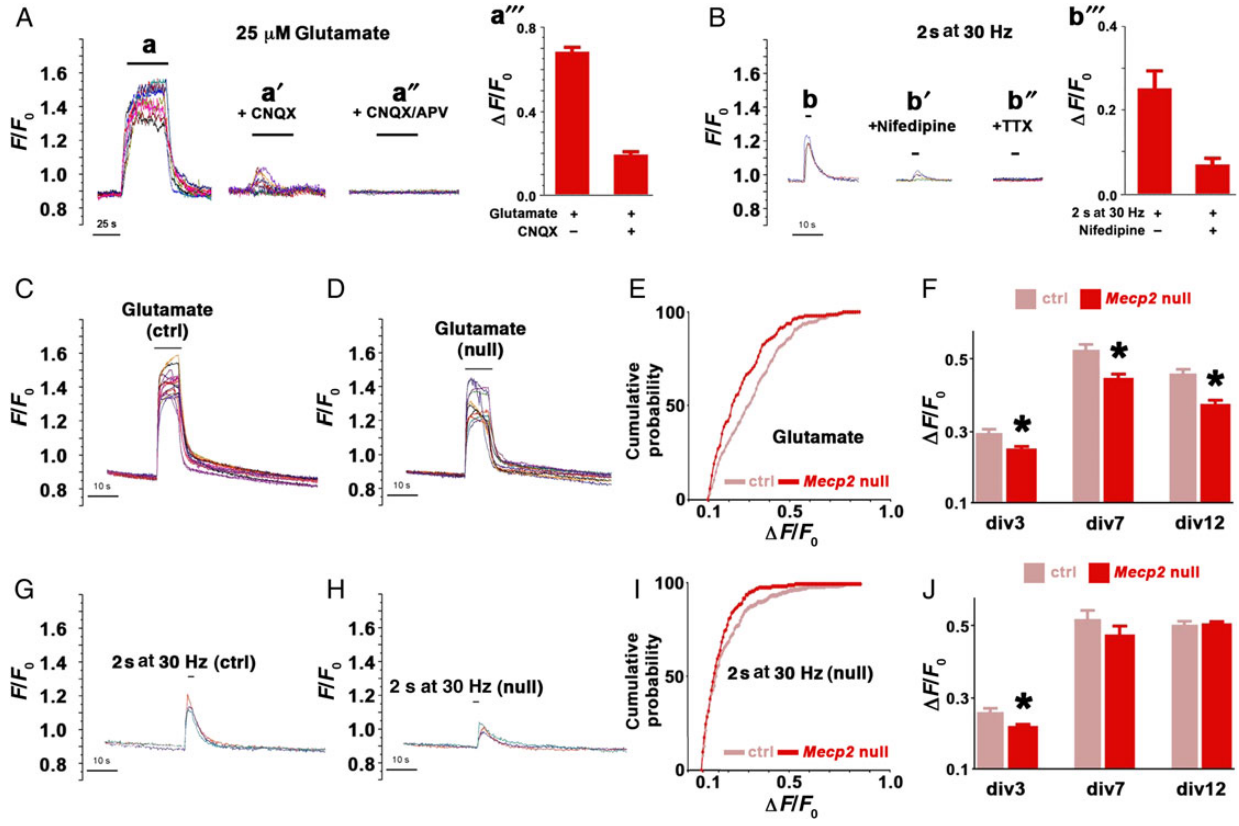

Figure 6. *Mecp2* null neurons exhibit lower calcium responses upon both glutamate and electrical stimulation. In *A*, temporal intracellular calcium changes are generated upon stimulation with 25 μM glutamate (a); in (*B*), calcium changes are generated by electrical field stimulation with a stimulus of 2 s at 30 Hz (b). Glutamate-mediated calcium responses were strongly reduced by adding 20 μM 6-cyano-7-nitroquinoxaline-2,3-dione (CNQX) (a′) and completely abolished with both 20 μM CNQX and 50 μM R-2-amino-5-phosphonopentanoate (APV) (a″), indicating that such calcium response was for the most part (75%) ascribable to the activation of AMPA receptors (a‴). Electrically evoked calcium responses performed in the presence of 50 μM APV, 20 μM CNQX, and 20 μM Bicuculline (b) were strongly reduced by 20 μM Nifedipine (b′) and completely abolished by 1 μM TTX (b″). Panel b‴ quantitatively depicts such effects. The analyses of calcium changes upon either glutamate (*C*–*F*) or electrical stimulation (*G*–*J*) were performed on wild type and *Mecp2* null neurons at different DIV (*F*–*J*, Supplementary Fig. 7; Supplementary Fig. 6 shows a representative field of view used for imaging calcium waves in neuronal cell body loaded with Oregon Green before and after either glutamate stimulation or electrical stimulation). Data depicted in (*E*) and (*I*) represent the cumulative analysis obtained at DIV3. Data in (*F*) and (*J*) represent the mean value of the ratio between ΔF and F_0 at different time points obtained, respectively, upon glutamate or electrical field stimulation (*$P < 0.05$ *t*-test).

In agreement with the transcriptional and GSEA results, indicating alterations of the levels of ionotropic glutamatergic receptors in *Mecp2* null neurons, a significantly lower response to glutamate was recorded in null neurons compared with wild type (Fig. 6*C–F*); interestingly, this decrease was maintained at both DIV7 and DIV12 (Supplementary Fig. 7*A*,*B*). Accordingly, measurements of neuronal calcium responsiveness evoked by a short-field electrical stimulation revealed that electrically evoked calcium responses (recorded at DIV3) were significantly lower in null neurons compared with wild type (Fig. 6*G–J*), thus confirming that maturing neurons lacking *Mecp2* exhibit a reduced neuronal responsiveness to electrical stimulation. These findings are clearly in line with the downregulation of genes encoding for both Na^+ and L-type Ca^{2+} channels depicted in Figures 4 and 5C. However, this feature was not maintained over time, as, by DIV7, wild type and null neurons responded in an overlapping manner to the electrical stimulation (Fig. 6*J* and Supplementary Fig. 7*C*,*D*).

To further validate the hypothesis that early defects in *Mecp2* expression affect the transcription of genes involved in activity-dependent signaling, we depleted *Mecp2* expression in wild type cortical neurons by electroporating in utero short hairpin sequences targeting *Mecp2* mRNA (Fig. 7). Given the low number of transduced neurons, this technique likely reveals cell autonomous effects of the gene knockdown.

E13.5 embryos from wild type timed-pregnant females were electroporated with either control (LacZ-directed short hairpin) or *Mecp2*-directed short hairpin (Zhou et al. 2006). Embryos were harvested at E18.5 and GFP-positive tissues were collected under a fluorescent stereoscope; GFP-positive neurons were then sorted from the GFP-negative internal controls. qPCR analyses on total RNA isolated from such cells confirmed the downregulation of *Mecp2* and the reduced expression of different AMPA and NMDA receptor subunits, as well as L-type Ca^{2+} (*Cacna1d* and *Cacng2*) and Na^+ channels (*Scn8a*) subunits, as depicted in Figure 7A.

It is known that the expression of proteins responsible for activity-dependent signaling, such as ion channels, neurotransmitter receptors, and Ca^{2+} channels, are critical for several aspects of neuronal maturation, including neuronal migration (Rakic and Komuro 1995; Komuro and Rakic 1998; Kumada and Komuro 2004). Such evidences prompted us to evaluate whether the transcriptional alteration observed in *Mecp2* shRNA-electroporated neurons might affect cortical neuronal migration in vivo. As expected, we found that control neurons (electroporated with LacZ-directed sh) mostly populated the upper portions of the CP, the physiological target for neurons born at E13.5 (Angevine and Sidman 1961; Rakic et al. 1974; Fig. 7*B*). Conversely, GFP-positive neurons electroporated at E13.5 with *Mecp2* shRNA mostly failed to properly migrate to the CP by E18.5, and rather, remained close to the VZ (Fig. 7C). The statistical evaluation of the migration of electroporated cells is depicted in Figure 7*D*. Given the transcriptional and migration defects depicted in Figure 7, we searched for a similar phenotype in *Mecp2* null mice. Thus, newly born neurons were BrdU-labeled at E13.5 and their migration was analyzed at E18.5; however, in these experimental conditions, migration of BrdU-positive neurons was similar in *Mecp2* null and wild type developing cortexes (Supplementary Fig. 5C).

Discussion

Many mouse models carrying different *Mecp2* alterations have been generated to improve our comprehension of MeCP2 functions and the mechanisms underlying RTT or other *MECP2*-related conditions (Bedogni et al. 2014). The use of such models demonstrated that: (1) the inactivation of *Mecp2* at different post-natal ages (from late juvenile to adult) always causes the appearance of severe neurological phenotypes and premature death (McGraw et al. 2011; Cheval et al. 2012; Nguyen et al. 2012) and (2) the MeCP2-related conditions are reversible at least in mice (Giacometti et al. 2007; Guy et al. 2007; Jugloff et al. 2008; Garg et al. 2013). However, in spite of these recent enormous advances, the knowledge regarding the temporal steps through which the consequences of dysfunctional MeCP2 activity begin to manifest is still limited. In fact, most studies have been performed in pre-symptomatic (3–6 weeks of age) or symptomatic (adult) male animals. Nonetheless, the presence of subtle but consistent impairments at early post-natal ages, when typical symptoms are not yet overt (Nomura 2005; Picker et al. 2006; Chao et al. 2007; Santos et al. 2007; Fehr et al. 2011), strongly indicates that also the maturing brain depends on MeCP2 activities.

At the molecular level, most of the data obtained so far suggest that *MECP2*-related pathologies might be associated with its direct or indirect involvement in gene expression regulation. Unfortunately, however, the outcomes of defective MeCP2

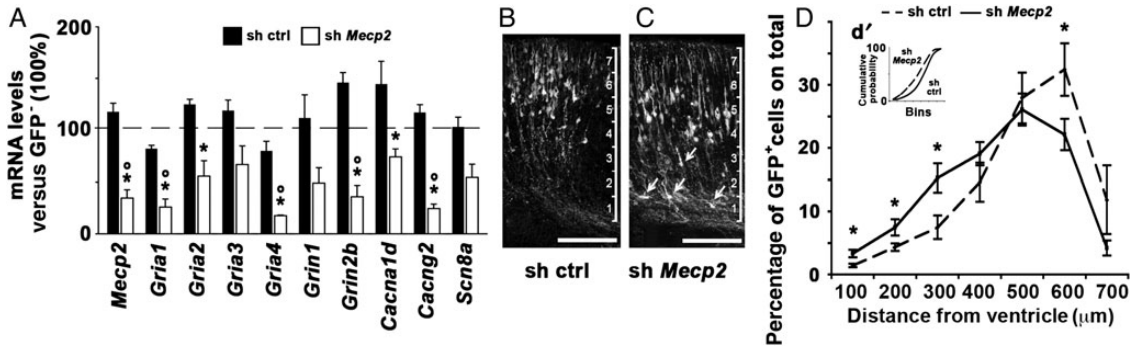

Figure 7. Acute reduction of Mecp2 downregulates gene expression and impairs neuronal migration in vivo. (A) Transcription of glutamatergic receptor and ionic channel subunits of sorted cells was measured through qPCR; data are expressed as the percentage of expression compared with non-electroporated (non-fluorescent) cells (100%, dotted line ± SEM). Two-way ANalysis Of VAriance (ANOVA) was followed by Bonferroni post hoc tests (°$P < 0.05$ vs. non-fluorescent controls; *$P < 0.05$ vs. LacZ sh; $N = 4$). (*B* and *C*) are representative images of the positioning of the GFP^+ cells in the cortex 5 days after electroporation. The graph in *D* was designed by considering the number of GFP^+ cells in each bin subdividing the cortical thickness over the total of GFP^+ cells counted for each animal. T-test was used to statistically verify the differences between groups in each bin (*$P < 0.05$). Both the 2 groups (*Mecp2* and *LacZ* sh) were composed of at least 8 different embryonic brains. The 2 cumulative distributions (in d′) were analyzed through the Kolmogorov–Smirnov test, revealing a divergence between the 2 groups of 17.8%, with a *P*-value <0.01. Scale bars: *B*, *C*: 100 μm.

activity are far from being understood and the identification of its specific transcriptional targets, especially at the early stages of the pathology, proved to be a difficult goal to achieve. Thus, we started off analyzing Mecp2 expression during embryonic maturation of the neocortex. The rationale was dual: first, the cortex has a clear involvement in MeCP2-related disorders (Armstrong 2001; Fukuda et al. 2005; Zhang et al. 2014); second, embryonic gene expression profile is a field only mildly approached in RTT that, however, should enable to avoid most if not all other indirect effects driven by either the health status of the animal or the environment. By superimposing microarray outputs to custom-made gene sets based on published data (Ayoub et al. 2011), we hypothesized that *Mecp2* null cortexes do not properly acquire the transcriptional signature of mature neurons in the E15.5 CP (Fig. 2). The immaturity of the transcriptional phenotype well correlates with the defective morphology displayed by null primary cortical neurons (Fig. 5), a feature that is in line with previous data highlighting maturation impairments in neurons derived from human RTT iPS cells (Marchetto et al. 2010; Walsh and Hochedlinger 2010; Kim et al. 2011; Farra et al. 2012; Dajani et al. 2013). Noticeably, our GSEA output clearly suggests that such defects are due to many modest but consistent transcriptional alterations affecting genes involved in related or unrelated molecular pathways.

GSEA revealed the downregulation of a large set of genes involved in the control of activity-dependent signaling pathways, which then mediate transcriptional, translational, and plasticity mechanisms. Among these, genes controlling activity-dependent Ca^{2+} signaling represent a pivotal pathway present throughout the entire life of a neuron and indeed, intracellular Ca^{2+} dynamics have been described as early as E13.5 in proliferating progenitors (Desarmenien and Spitzer 1991; Gu and Spitzer 1995; LoTurco et al. 1995; Spitzer 2006), migrating neurons (Komuro and Rakic 1998; Behar et al. 1999; Spitzer 2006), and post-mitotic neurons (Platel et al. 2005). Moreover, it has also been reported that spontaneous neuronal activity contributing to maturation and refinement of neuronal circuits occurs in several brain regions at embryonic stages, including retina, thalamus, and cortex, thus even before experience-dependent activity driven by external sensory input (Meister et al. 1991; Yuste et al. 1992; Galli and Maffei 1998; Feller 1999; Weliky and Katz 1999). Given that *Mecp2* null primary cortical neurons established at E15.5 exhibit lower calcium responsiveness to both glutamate and electrical stimuli at early stages of development, it is reasonable to hypothesize that early defects in neuronal excitability might play a critical role in the altered neuronal maturation observed during adulthood in different *Mecp2* null models.

The ability of a neuronal cell to exhibit proper spontaneous activity and to respond to external stimuli reflects its stage of maturation; nonetheless, and more intriguingly, this ability is obviously part of the mechanisms through which a neuron differentiates during early development and functions later in adulthood. Accordingly, the defects described here are in line with the recently discovered morphological defects displayed by *Mecp2* null neurons at DIV4 (Baj et al. 2014); importantly, they largely precede the onset of neurological outcomes in *Mecp2* animal models. A tight link between early neuronal activity and late maturation of synaptic contacts has been shown both in vivo (Lin et al. 2010; Uchino et al. 2010) and in vitro (Perlini et al. 2011; Andreae and Burrone 2014). In fact, neuronal activity, through local and global changes of several activity-dependent signaling pathways, plays an important role not only during early phases of proliferation, migration, and differentiation but also at later stages of development, during synapse formation, and neuronal survival (Komuro and Rakic 1998; Crair 1999; Zhang and Poo 2001; Luján et al. 2005; Spitzer 2006; Rosenberg and Spitzer 2011). Therefore, our results likely foreshadow the reduction in the number of synapses in cultured *Mecp2* null neurons compared with wild type, thereby linking transcriptional effects responsible for the reduced neuronal activity (this work) with altered synaptogenesis (Chao et al. 2007; Cohen and Greenberg 2008). Our observations are of particular interest in light of the recent hypothesis that several syndromes, including autism spectrum disorders, X-fragile, tuberous sclerosis, and Angelman syndrome, are all characterized by common alterations in the activity-dependent signaling networks controlling proper structural maturation of the brain (Ebert and Greenberg 2013). Intriguingly, the downstream effects of such alterations would likely lead to alterations in brain connectivity, a classical feature of RTT (Kishi and Macklis 2004; Degano et al. 2009).

Given the virtual lack of glial cells in both early in vivo and in vitro conditions, the low density neuronal seeding delaying the formation of contacts between neurons, and the early developmental stage at which calcium transients are recorded (DIV3), it is reasonable to infer that the link between the transcriptional defects and the intrinsic maturation impairments displayed by *Mecp2* null neurons most likely arises from cell autonomous mechanisms. This is confirmed by the overlapping transcriptional alterations displayed by full null embryonic cortexes and *Mecp2* silenced neurons sorted from otherwise normal cortical cells (Fig. 7A). Our observations are thus in agreement with the data presented by Kishi and Macklis (2010), in which the authors elegantly demonstrated that the transplantation of *Mecp2* null projection neurons into wild type cortex does not prevent or rescue their impairments in morphology and complexity of dendritic structures. Of note, a reduced nuclear size was highlighted in young cultured null neurons, whereas E18.5 brain sections only displayed a non-significant tendency to nuclear size reduction, a typical feature of *MeCP2*-deficient adult neurons. Accordingly, we observed migration defects in the restricted cohort of cells depleted of *Mecp2* through in utero electroporation, but not in null cortical tissues. We speculate that compensatory mechanisms might mask or even partly rescue defects that are evident only when analyzed in conditions enabling cell autonomous studies.

To conclude, our data suggest that newborn *Mecp2* null cortical neurons display critical transcriptional defects that lead to reduced neuronal responsiveness, which, in turn, delays and disrupts proper neuronal maturation. Although we cannot rule out that other mechanisms could later determine at least a partial rescue of the phenotype here described, we speculate that the neurological phenotype displayed by *Mecp2* null animals and RTT patients could thus be the cumulative result of different adverse events occurring ever since early embryonic maturation through either cell autonomous or non-autonomous mechanisms. Accordingly, it is well described that *Mecp2* null glia and microglia, cell types continuously going through cycles of turnover and maturation throughout life, have detrimental effects on neuronal functionality due to their inability to exert trophic support (Ballas et al. 2009; Lioy et al. 2011; Derecki et al. 2012, 2013; Zeidán-Chuliá et al. 2014). Moreover, given the ubiquitous expression of *Mecp2* in many different cell types, maturation defects could occur outside the brain as well, and contribute to other RTT non-neurological features.

Supplementary Material

Supplementary material can be found at http://www.cercor.oxfordjournals.org/ online

Funding

Grant resources are as follows: Fondazione Cariplo (Grant 2010-0724 to N.L.); Fondazione Telethon (Grant GGP10032 to N.L.); Jerome Lejeune Foundation (to F.B.); ERC Consolidator Grant (617978 to M.P.); Health F2-2009-241498 Eurospin (to M.M.).

Notes

We are very thankful to ProRett Ricerca, an association of Italian parents of RTT girls whose efforts represent our major source of both strive and funding. F.B. and N.L. thank Vania Broccoli and his co-workers for kindly sharing reagents and knowledge. *Conflict of Interest*: None declared.

References

Amir RE, Van den Veyver IB, Wan M, Tran CQ, Francke U, Zoghbi HY. 1999. Rett syndrome is caused by mutations in X-linked MECP2, encoding methyl-CpG-binding protein 2. Nat Genet. 23(2):185–188.

Andreae LC, Burrone J. 2014. The role of neuronal activity and transmitter release on synapse formation. Curr Opin Neurobiol. 27:47–52.

Angevine JB Jr, Sidman RL. 1961. Autoradiographic study of cell migration during histogenesis of cerebral cortex in the mouse. Nature. 192:766–768.

Armstrong DD. 2001. Rett syndrome neuropathology review 2000. Brain Dev. 23(Suppl 1):S72–S76.

Asaka Y, Jugloff DG, Zhang L, Eubanks JH, Fitzsimonds RM. 2006. Hippocampal synaptic plasticity is impaired in the Mecp2-null mouse model of Rett syndrome. Neurobiol Dis. 21(1):217–227.

Ayoub AE, Oh S, Xie Y, Leng J, Cotney J, Dominguez MH, Noonan JP, Rakic P. 2011. Transcriptional programs in transient embryonic zones of the cerebral cortex defined by high-resolution mRNA sequencing. Proc Natl Acad Sci USA. 108 (36):14950–5.

Baj G, Patrizio A, Montalbano A, Sciancalepore M, Tongiorgi E. 2014. Developmental and maintenance defects in Rett syndrome neurons identified by a new mouse staging system in vitro. Front Cell Neurosci. 8:18.

Ballas N, Lioy DT, Grunseich C, Mandel G. 2009. Non-cell autonomous influence of MeCP2-deficient glia on neuronal dendritic morphology. Nat Neurosci. 12(3):311–317.

Bedogni F, Rossi RL, Galli F, Cobolli Gigli C, Gandaglia A, Kilstrup-Nielsen C, Landsberger N. 2014. Rett syndrome and the urge of novel approaches to study MeCP2 functions and mechanisms of action. Neurosci Biobehav Rev. 46 Pt 2:187–201.

Behar TN, Scott CA, Green CL, Wen X, Smith SV, Maric D, Liu QY, Colton CA, Barker JL. 1999. Glutamate acting at NMDA receptors stimulates embryonic cortical neuronal migration. J Neurosci. 19(11):4449–4461.

Belichenko NP, Belichenko PV, Li HH, Mobley WC, Francke U. 2008. Comparative study of brain morphology in Mecp2 mutant mouse models of Rett syndrome. J Comp Neurol. 508(1):184–195.

Belichenko PV, Wright EE, Belichenko NP, Masliah E, Li HH, Mobley WC, Francke U. 2009. Widespread changes in dendritic and axonal morphology in Mecp2-mutant mouse models of Rett syndrome: evidence for disruption of neuronal networks. J Comp Neurol. 514(3):240–258.

Bienvenu T, Carrié A, de Roux N, Vinet MC, Jonveaux P, Couvert P, Villard L, Arzimanoglou A, Beldjord C, Fontes M, et al. 2000. MECP2 mutations account for most cases of typical forms of Rett syndrome. Hum Mol Genet. 9(9):1377–1384.

Caballero I, Hansen J, Leaford D, Pollard S, Hendrich BD. 2009. The methyl-CpG binding proteins Mecp2, Mbd2 and Kaiso are dispensable for mouse embryogenesis, but play a redundant function in neural differentiation. PLoS ONE. 4(1): e4315.

Chao HT, Zoghbi HY, Rosenmund C. 2007. MeCP2 controls excitatory synaptic strength by regulating glutamatergic synapse number. Neuron. 56(1):58–65.

Chen RZ, Akbarian S, Tudor M, Jaenisch R. 2001. Deficiency of methyl-CpG binding protein-2 in CNS neurons results in a Rett-like phenotype in mice. Nat Genet. 27(3):327–331.

Cheval H, Guy J, Merusi C, De Sousa D, Selfridge J, Bird A. 2012. Postnatal inactivation reveals enhanced requirement for MeCP2 at distinct age windows. Hum Mol Genet. 21(17): 3806–3814.

Cohen S, Greenberg ME. 2008. Communication between the synapse and the nucleus in neuronal development, plasticity, and disease. Annu Rev Cell Dev Biol. 24:183–209.

Crair MC. 1999. Neuronal activity during development: permissive or instructive? Curr Opin Neurobiol. 9(1):88–93.

Dajani R, Koo SE, Sullivan GJ, Park IH. 2013. Investigation of Rett syndrome using pluripotent stem cells. J Cell Biochem. 114 (11):2446–2453.

Degano AL, Pasterkamp RJ, Ronnett GV. 2009. MeCP2 deficiency disrupts axonal guidance, fasciculation, and targeting by altering Semaphorin 3F function. Mol Cell Neurosci. 42(3): 243–254.

Della Sala G, Pizzorusso T. 2014. Synaptic plasticity and signaling in Rett syndrome. Dev Neurobiol. 74(2):178–196.

Derecki NC, Cronk JC, Kipnis J. 2013. The role of microglia in brain maintenance: implications for Rett syndrome. Trends Immunol. 34(3):144–150.

Derecki NC, Cronk JC, Lu Z, Xu E, Abbott SB, Guyenet PG, Kipnis J. 2012. Wild-type microglia arrest pathology in a mouse model of Rett syndrome. Nature. 484(7392):105–109.

Desarmenien MG, Spitzer NC. 1991. Role of calcium and protein kinase C in development of the delayed rectifier potassium current in Xenopus spinal neurons. Neuron. 7(5):797–805.

Ebert DH, Greenberg ME. 2013. Activity-dependent neuronal signalling and autism spectrum disorder. Nature. 493(7432): 327–337.

Englund C, Fink A, Lau C, Pham D, Daza RA, Bulfone A, Kowalczyk T, Hevner RF. 2005. Pax6, Tbr2, and Tbr1 are expressed sequentially by radial glia, intermediate progenitor cells, and postmitotic neurons in developing neocortex. J Neurosci. 25(1):247–251.

Farra N, Zhang WB, Pasceri P, Eubanks JH, Salter MW, Ellis J. 2012. Rett syndrome induced pluripotent stem cell-derived neurons reveal novel neurophysiological alterations. Mol Psychiatry. 17(12):1261–1271.

Fehr S, Bebbington A, Ellaway C, Rowe P, Leonard H, Downs J. 2011. Altered attainment of developmental milestones influences the age of diagnosis of Rett syndrome. J Child Neurol. 26(8):980–987.

Feller MB. 1999. Spontaneous correlated activity in developing neural circuits. Neuron. 22(4):653–656.

Fu F, Liu HL, Li R, Han J, Yang X, Min P, Zhen L, Zhang YL, Xie GE, Ying LT, et al. 2014. Prenatal diagnosis of fetuses with congenital abnormalities and duplication of the MECP2 region. Gene. 546(2):222–225.

Fukuda T, Itoh M, Ichikawa T, Washiyama K, Goto Y. 2005. Delayed maturation of neuronal architecture and synaptogenesis in cerebral cortex of Mecp2-deficient mice. J Neuropathol Exp Neurol. 64(6):537–544.

Fyffe SL, Neul JL, Samaco RC, Chao HT, Ben-Shachar S, Moretti P, McGill BE, Goulding EH, Sullivan E, Tecott LH, et al. 2008. Deletion of Mecp2 in Sim1-expressing neurons reveals a critical role for MeCP2 in feeding behavior, aggression, and the response to stress. Neuron. 59(6):947–958.

Galli L, Maffei L. 1998. Spontaneous impulse activity of rat retinal ganglion cells in prenatal life. Science. 242(4875):90–91.

Garg SK, Lioy DT, Cheval H, McGann JC, Bissonnette JM, Murtha MJ, Foust KD, Kaspar BK, Bird A, Mandel G 2013. Systemic delivery of MeCP2 rescues behavioral and cellular deficits in female mouse models of Rett syndrome. J Neurosci. 33 (34):13612–13620.

Gemelli T, Berton O, Nelson ED, Perrotti LI, Jaenisch R, Monteggia LM. 2006. Postnatal loss of methyl-CpG binding protein 2 in the forebrain is sufficient to mediate behavioral aspects of Rett syndrome in mice. Biol Psychiatry. 59(5): 468–476.

Giacometti E, Luikenhuis S, Beard C, Jaenisch R. 2007. Partial rescue of MeCP2 deficiency by postnatal activation of MeCP2. Proc Natl Acad Sci USA. 104(6):1931–1936.

Gritti A, Parati EA, Cova L, Frolichsthal P, Galli R, Wanke E, Faravelli L, Morassutti DJ, Roisen F, Nickel DD, et al. 1996. Multipotential stem cells from the adult mouse brain proliferate and self-renew in response to basic fibroblast growth factor. J Neurosci. 16(3):1091–1100.

Gu X, Spitzer NC. 1995. Distinct aspects of neuronal differentiation encoded by frequency of spontaneous Ca^{2+} transients. Nature. 375(6534):784–787.

Guo ZY, Li CZ, Li XJ, Wang YL, Mattson MP, Lu CB. 2013. The developmental regulation of glutamate receptor-mediated calcium signaling in primary cultured rat hippocampal neurons. Neuroreport. 24(9):492–497.

Guy J, Hendrich B, Holmes M, Martin JE, Bird A. 2001. A mouse Mecp2-null mutation causes neurological symptoms that mimic Rett syndrome. Nat Genet. 27(3):322–326.

Guy J, Gan J, Selfridge J, Cobb S, Bird A. 2007. Reversal of neurological defects in a mouse model of Rett syndrome. Science. 315(5815):1143–1147.

Jugloff DG, Vandamme K, Logan R, Visanji NP, Brotchie JM, Eubanks JH 2008. Targeted delivery of an Mecp2 transgene to forebrain neurons improves the behavior of female Mecp2-deficient mice. Hum Mol Genet. 17(10):1386–1396.

Jung BP, Jugloff DG, Zhang G, Logan R, Brown S, Eubanks JH. 2003. The expression of methyl CpG binding factor MeCP2 correlates with cellular differentiation in the developing rat brain and in cultured cells. J Neurobiol. 55(1):86–96.

Kim KY, Hysolli E, Park IH. 2011. Neuronal maturation defect in induced pluripotent stem cells from patients with Rett syndrome. Proc Natl Acad Sci USA. 108(34):14169–14174.

Kishi N, Macklis JD. 2010. MeCP2 functions largely cell-autonomously, but also non-cell-autonomously, in neuronal maturation and dendritic arborization of cortical pyramidal neurons. Exp Neurol. 222(1):51–58.

Kishi N, Macklis JD. 2004. MECP2 is progressively expressed in post-migratory neurons and is involved in neuronal maturation rather than cell fate decisions. Mol Cell Neurosci. 27 (3):306–321.

Komuro H, Rakic P. 1998. Orchestration of neuronal migration by activity of ion channels, neurotransmitter receptors, and intracellular Ca^{2+} fluctuations. J Neurobiol. 37(1):110–130.

Kumada T, Komuro H. 2004. Completion of neuronal migration regulated by loss of Ca(2+) transients. Proc Natl Acad Sci USA. 101(22):8479–8484.

Li H, Zhong X, Chau KF, Williams EC, Chang Q. 2011. Loss of activity-induced phosphorylation of MeCP2 enhances synaptogenesis, LTP and spatial memory. Nat Neurosci. 14(8): 1001–1008.

Lin CW, Sim S, Ainsworth A, Okada M, Kelsch W, Lois C. 2010. Genetically increased cell-intrinsic excitability enhances neuronal integration into adult brain circuits. Neuron. 65 (1):32–39.

Lioy DT, Garg SK, Monaghan CE, Raber J, Foust KD, Kaspar BK, Hirrlinger PG, Kirchhoff F, Bissonnette JM, Ballas N, et al. 2011. A role for glia in the progression of Rett's syndrome. Nature. 475(7357):497–500.

LoTurco JJ, Owens DF, Heath MJ, Davis MB, Kriegstein AR. 1995. GABA and glutamate depolarize cortical progenitor cells and inhibit DNA synthesis. Neuron. 15(6):1287–1298.

Luján R, Shigemoto R, López-Bendito G. 2005. Glutamate and GABA receptor signalling in the developing brain. Neuroscience. 130(3):567–580.

Magri L, Cambiaghi M, Cominelli M, Alfaro-Cervello C, Cursi M, Pala M, Bulfone A, Garcìa-Verdugo JM, Leocani L, Minicucci F, et al. 2011. Sustained activation of mTOR pathway in embryonic neural stem cells leads to development of tuberous sclerosis complex-associated lesions. Cell Stem Cell. 9(5): 447–462.

Marchetto MC, Carromeu C, Acab A, Yu D, Yeo GW, Mu Y, Chen G, Gage FH, Muotri AR. 2010. A model for neural development and treatment of Rett syndrome using human induced pluripotent stem cells. Cell. 143(4):527–539.

McGraw CM, Samaco RC, Zoghbi HY. 2011. Adult neural function requires MeCP2. Science. 333(6039):186.

Miralvès J, Magdeleine E, Joly E. 2007. Design of an improved set of oligonucleotide primers for genotyping MeCP2tm1.1Bird KO mice by PCR. Mol Neurodegener. 2:16.

Meister M, Wong RO, Baylor DA, Shatz CJ. 1991. Synchronous bursts of action potentials in ganglion cells of the developing mammalian retina. Science. 252(5008):939–943.

Nguyen MV, Du F, Felice CA, Shan X, Nigam A, Mandel G, Robinson JK, Ballas N. 2012. MeCP2 is critical for maintaining mature neuronal networks and global brain anatomy during late stages of postnatal brain development and in the mature adult brain. J Neurosci. 32(29):10021–10034.

Nomura Y. 2005. Early behavior characteristics and sleep disturbance in Rett syndrome. Brain Dev. 27(Suppl 1):S35–S42.

Okabe Y, Kusaga A, Takahashi T, Mitsumasu C, Murai Y, Tanaka E, Higashi H, Matsuishi T, Kosai K. 2010. Neural development of methyl-CpG-binding protein 2 null embryonic stem cells: a system for studying Rett syndrome. Brain Res. 1360:17–27.

Perlini LE, Botti F, Fornasiero EF, Giannandrea M, Bonanomi D, Amendola M, Naldini L, Benfenati F, Valtorta F. 2011. Effects of phosphorylation and neuronal activity on the control of synapse formation by synapsin I. J Cell Sci. 124(Pt 21):3643–3653.

Picker JD, Yang R, Ricceri L, Berger-Sweeney J. 2006. An altered neonatal behavioral phenotype in Mecp2 mutant mice. Neuroreport. 17(5):541–544.

Platel JC, Boisseau S, Dupuis A, Brocard J, Poupard A, Savasta M, Villaz M, Albrieux M. 2005. Na^{+} channel-mediated Ca^{2+} entry leads to glutamate secretion in mouse neocortical preplate. Proc Natl Acad Sci USA. 102(52):19174–9.

Pozzi D, Lignani G, Ferrea E, Contestabile A, Paonessa F, D'Alessandro R, Lippiello P, Boido D, Fassio A, Meldolesi J, et al. 2013. REST/NRSF-mediated intrinsic homeostasis protects neuronal networks from hyperexcitability. EMBO J. 32 (22):2994–3007.

Pravettoni E, Bacci A, Coco S, Forbicini P, Matteoli M, Verderio C. 2000. Different localizations and functions of L-type and N-type calcium channels during development of hippocampal neurons. Dev Biol. 227(2):581–594.

Rakic P, Komuro H. 1995. The role of receptor/channel activity in neuronal cell migration. J Neurobiol. 26(3):299–315.

Rakic P, Stensas LJ, Sayre E, Sidman RL. 1974. Computer-aided three-dimensional reconstruction and quantitative analysis of cells from serial electron microscopic montages of foetal monkey brain. Nature. 250(461):31–34.

Ricceri L, De Filippis B, Laviola G. 2008. Mouse models of Rett syndrome: from behavioural phenotyping to preclinical evaluation of new therapeutic approaches. Behav Pharmacol. 19 (5–6):501–517.

Rosenberg SS, Spitzer NC. 2011. Calcium signaling in neuronal development. Cold Spring Harb Perspect Biol. 3(10):a004259.

Santos M, Silva-Fernandes A, Oliveira P, Sousa N, Maciel P. 2007. Evidence for abnormal early development in a mouse model of Rett syndrome. Genes Brain Behav. 6(3):277–286.

Schmid RS, Tsujimoto N, Qu Q, Lei H, Li E, Chen T, Blaustein CS. 2008. A methyl-CpG-binding protein 2-enhanced green fluorescent protein reporter mouse model provides a new tool for studying the neuronal basis of Rett syndrome. Neuroreport. 19 (4):393–398.

Schüle B, Armstrong DD, Vogel H, Oviedo A, Francke U. 2008. Severe congenital encephalopathy caused by MECP2 null mutations in males: central hypoxia and reduced neuronal dendritic structure. Clin Genet. 74(2):116–126.

Smrt RD, Eaves-Egenes J, Barkho BZ, Santistevan NJ, Zhao C, Aimone JB, Gage FH, Zhao X. 2007. Mecp2 deficiency leads to delayed maturation and altered gene expression in hippocampal neurons. Neurobiol Dis. 27(1):77–89.

Spitzer NC. 2006. Electrical activity in early neuronal development. Nature. 444(7120):707–712.

Subramanian A, Tamayo P, Mootha VK, Mukherjee S, Ebert BL, Gillette MA, Paulovich A, Pomeroy SL, Golub TR, Lander ES, et al. 2005. Gene set enrichment analysis: a knowledge-based approach for interpreting genome-wide expression profiles. Proc Natl Acad Sci USA. 102(43):15545–15550.

Uchino S, Hirasawa T, Tabata H, Gonda Y, Waga C, Ondo Y, Nakajima K, Kohsaka S. 2010. Inhibition of *N*-methyl-D-aspartate receptor activity resulted in aberrant neuronal migration caused by delayed morphological development in the mouse neocortex. Neuroscience. 169(2):609–618.

Yuste R, Peinado A, Katz LC. 1992. Neuronal domains in developing neocortex. Science. 257(5070):665–669.

Walsh RM, Hochedlinger K. 2010. Modeling Rett syndrome with stem cells. Cell. 143(4):499–500.

Weliky M, Katz LC. 1999. Correlational structure of spontaneous neuronal activity in the developing lateral geniculate nucleus in vivo. Science. 285(5427):599–604.

Yusufzai TM, Wolffe AP. 2000. Functional consequences of Rett syndrome mutations on human MeCP2. Nucleic Acids Res. 28(21):4172–4179.

Zeidán-Chuliá F, Salmina AB, Malinovskaya NA, Noda M, Verkhratsky A, Moreira JC. 2014. The glial perspective of autism spectrum disorders. Neurosci Biobehav Rev. 38:160–172.

Zhang L, He J, Jugloff DG, Eubanks JH. 2008. The MeCP2-null mouse hippocampus displays altered basal inhibitory rhythms and is prone to hyperexcitability. Hippocampus. 18(3): 294–309.

Zhang LI, Poo MM. 2001. Electrical activity and development of neural circuits. Nat Neurosci. 4(Suppl):1207–1214.

Zhang W, Peterson M, Beyer B, Frankel WN, Zhang ZW. 2014. Loss of MeCP2 from forebrain excitatory neurons leads to cortical hyperexcitation and seizures. J Neurosci. 34 (7):2754–2763.

Zhou Z, Hong EJ, Cohen S, Zhao WN, Ho HY, Schmidt L, Chen WG, Lin Y, Savner E, Griffith EC, et al. 2006. Brain-specific phosphorylation of MeCP2 regulates activity-dependent Bdnf transcription, dendritic growth, and spine maturation. Neuron. 52 (2):255–269.